1-1-2008

Numb Endocytic adapter proteins regulate the transport and processing of the amyloid precursor protein in an isoform-dependent manner - Implications for Alzheimer disease pathogenesis

George A. Kyriazis
University of Central Florida

Zelan Wei
University of Central Florida

Miriam Vandermey
University of Central Florida

Dong-Gyu Jo
Ouyang Xin

See next page for additional authors

THE JOURNAL OF BIOLOGICAL CHEMISTRY VOL. 283, NO. 37, pp. 25492–25502, September 12, 2008
Printed in the U.S.A.

Numb Endocytic Adapter Proteins Regulate the Transport and Processing of the Amyloid Precursor Protein in an Isoform-dependent Manner

IMPLICATIONS FOR ALZHEIMER DISEASE PATHOGENESIS[*][S]

Received for publication, March 14, 2008, and in revised form, July 1, 2008 Published, JBC Papers in Press, July 2, 2008, DOI 10.1074/jbc.M802072200

George A. Kyriazis[‡], Zelan Wei[‡], Miriam Vandermey[‡], Dong-Gyu Jo[§], Ouyang Xin[¶], Mark P. Mattson[¶], and Sic L. Chan[‡1]

From the [‡]Biomolecular Science Center, University of Central Florida, Orlando, Florida 32816, the [§]College of Pharmacy, Sungkyunkwan University, Suwon 440-746, Korea, and the [¶]Laboratory of Neurosciences, NIA, National Institutes of Health, Intramural Research Program, Baltimore, Maryland 21224

Central to the pathogenesis of Alzheimer disease is the aberrant processing of the amyloid precursor protein (APP) to generate amyloid β-peptide (Aβ), the principle component of amyloid plaques. The cell fate determinant Numb is a phosphotyrosine binding domain (PTB)-containing endocytic adapter protein that interacts with the carboxyl-terminal domain of APP. The physiological relevance of this interaction is unknown. Mammals produce four alternatively spliced variants of Numb that differ in the length of their PTB and proline-rich region. In the current study, we determined the influence of the four human Numb isoforms on the intracellular trafficking and processing of APP. Stable expression of Numb isoforms that differ in the PTB but not in the proline-rich region results in marked differences in the sorting of APP to the recycling and degradative pathways. Neural cells expressing Numb isoforms that lack the insert in the PTB (short PTB (SPTB)) exhibited marked accumulation of APP in Rab5A-labeled early endosomal and recycling compartments, whereas those expressing isoforms with the insertion in the PTB (long PTB (LPTB)) exhibited reduced amounts of cellular APP and its proteolytic derivatives relative to parental control cells. Neither the activities of the β- and γ-secretases nor the expression of APP mRNA were significantly different in the stably transfected cells, suggesting that the differential effects of the Numb proteins on APP metabolism is likely to be secondary to altered APP trafficking. In addition, the expression of SPTB-Numb increases at the expense of LPTB-Numb in neuronal cultures subjected to stress, suggesting a role for Numb in stress-induced Aβ production. Taken together, these results suggest distinct roles for the human Numb isoforms in APP metabolism and may provide a novel potential link between altered Numb isoform expression and increased Aβ generation.

The amyloid precursor protein (APP)[2] is an integral transmembrane glycoprotein that is highly expressed in the brain and plays an important role in neuronal function (1). The abnormal processing of APP to generate the amyloid β-peptide (Aβ) leads to the extracellular neuritic plaques characteristic of Alzheimer disease (AD) (1–3). The rate of Aβ production is believed to be a key determinant of the onset and progression of AD. Although proteolytic processing of APP and characterization of the APP-cleaving enzymes (α-, β-, and γ-secretases) have revealed important targets for drug discovery, the regulation of APP trafficking is less well understood. Several recent findings support the idea that the intracellular transport and subcellular localization of APP are crucial determinants of APP processing and Aβ generation (4, 5). One pathway for Aβ generation involves the reinternalization of membrane-bound full-length APP (4, 5). Endosomes have been shown to be intracellular compartments, where the sequential action of β- and γ-secretases generates amyloidogenic COOH-terminal fragments of APP (APP-CTFs) and Aβ (1–3). APP is also targeted to and degraded in the lysosomes (6). On the other hand, cleavage within the Aβ region of APP by α-secretase, which prevents the production of Aβ, occurs in a late compartment of the secretory pathway, such as the Golgi, or at the cell surface (7). Deletion of the APP cytoplasmic tail or inhibition of endocytosis has been shown to reduce Aβ levels, suggesting that endocytosis is critical for Aβ generation (4, 5, 8). Understanding the mechanisms that regulate APP trafficking to distinct subcellular compartments with the different secretase activities is important for developing strategies to reduce abnormal processing and to prevent Aβ-induced neurotoxicity.

Numb is an evolutionarily conserved protein identified by its ability to control cell fate in the nervous system of *Dro-*

[S] The on-line version of this article (available at http://www.jbc.org) contains supplemental Fig. 1.

[1] To whom correspondence should be addressed: Burnett School of Biomedical Sciences, University of Central Florida, 4000 Central Florida Blvd., Orlando 32816. Tel.: 407-823-1354; Fax: 407-823-0956; E-mail: schan@mail.ucf.edu.

[2] The abbreviations used are: APP, amyloid precursor protein; Aβ, amyloid β-peptide; AD, Alzheimer disease; APP-CTF, COOH-terminal fragment of APP; PTB, phosphotyrosine binding domain; PRR, proline-rich region; SPTB, short PTB; LPTB, long PTB; ELISA, enzyme-linked immunosorbent assay; TFW, trophic factor withdrawal; PBS, phosphate-buffered saline; Tricine, *N*-[2-hydroxy-1,1-bis(hydroxymethyl)ethyl]glycine; sAPP, soluble APP; ANOVA, analysis of variance; TfR, transferrin receptor; E3, ubiquitin-protein isopeptide ligase; dyn, dynamin.

sophila (11, 12). Numb contains two protein-protein interaction domains, a phosphotyrosine-binding domain (PTB) and a proline-rich region (PRR) that functions as an Src homology 3-binding domain (13, 14). Although only one form of Numb has been identified in *Drosophila*, mammals produce four alternatively spliced variants of Numb that differ in the length of their PTB (lacking or containing an 11-amino acid insert) and PRR (lacking or containing a 48-amino acid insert) domains (13, 14). All Numb proteins contain the NPF (asparagine-proline-phenylalanine) and DPF (aspartate-proline-phenylalanine) motifs that are critical for interaction with proteins containing the Eps15 homology domain and with the clathrin protein AP-2, respectively. Numb can associate with clathrin-coated pits, vesicles, and endosomes, suggesting that it functions as an endocytic adapter protein (15, 16). Numb plays a role in the internalization of receptors that are involved not only in cell fate decisions during central nervous system development (17) but also in neuronal maturation, differentiation, and survival (18, 19). Notch is an evolutionarily conserved transmembrane receptor that specifies cell fate in a wide variety of tissues and organisms through local cell-cell interaction (20). Numb regulates the endocytic and ubiquitin-dependent processing of Notch (21) and consequently the cell fate decisions determined by Notch signaling (22, 23). In maturing neurons, Numb binds to the neural adhesion protein L1 and integrin in axonal growth cones and promotes their recycling (24, 25).

Previous work has demonstrated an interaction between APP and Numb in mouse brain lysates and in cell culture (26). Truncation and site-directed mutagenesis studies have shown that Numb binds to the YENPTY motif within the intracellular domain of APP (26). Several other APP binding partners that interact with this motif, including X11, Fe65, mDab, C-Abl, and JIP-1, have been demonstrated to affect endogenous APP localization and processing (27). Considering that Numb is an endocytic adapter protein, we determined whether expression of Numb influences the trafficking and processing of APP. Our results show that expression of Numb isoforms lacking the insert in the PTB (short PTB (SPTB)-Numb) caused the abnormal accumulation of cellular APP in the early endosomes and increased the levels of APP-CTFs. By contrast, expression of the Numb isoforms with the insert in PTB (long PTB (LPTB)-Numb) causes a significant reduction in the cellular content of APP and APP-CTFs. Interestingly, when cultured primary cortical neurons were subjected to trophic factor deprivation, the expression of the SPTB-Numb increased at the expense of LPTB-Numb, suggesting that pathophysiological conditions can alter Numb isoform expression in a manner that increases amyloidogenic processing of APP. Understanding the function of Numb in the trafficking of APP may provide insights into the regulation of APP processing in AD pathogenesis and lead to possible AD therapies.

EXPERIMENTAL PROCEDURES

Antibodies and Reagents—Antibodies used for immunodetection of APP were 6E10 (anti-Aβ 1–17) and 22C11 (anti-sAPPα) (Chemicon), anti-amino terminus of APP (2.F2.19B4; Chemicon), anti-carboxyl terminus of APP (APP 643–695), and 4G8 anti-Aβ (17–24) (Signet). The polyclonal antibodies to Numb were obtained from Santa Cruz Biotechnology, Inc. (Santa Cruz, CA) (sc-15590) or Upstate Biotechnology, Inc. (anti-pan-Numb). The antibodies to Rab proteins were Rab5a (Santa Cruz Biotechnology), Rab4a (Santa Cruz Biotechnology), Rab11 (Santa Cruz Biotechnology), and Rab7 (Sigma). LAMP-1 antibody was from Santa Cruz Biotechnology. Antibodies to the following tags were GST (glutathione *S*-transferase; Cell Signaling), hemagglutinin epitope (Santa Cruz Biotechnology), and FLAG epitope (Cell Signaling). Other antibodies included ERK1/2 and phospho-ERK1/2 (Cell Signaling), dynamin 1 (BD Biosciences), actin (Sigma), ubiquitin (P4D1; Santa Cruz Biotechnology), transferrin receptor (Zymed Laboratories Inc.), β-secretase 1 (BACE1; Sigma), presenilin-1 (PS1; Chemicon), nicastrin (Sigma), Aph-1 (Sigma), and Pen-2 (Santa Cruz Biotechnology). Immunofluorescence-conjugated secondary antibodies (Alexa Fluor 488-conjugated goat anti-mouse and Alexa Fluor 594-conjugated rabbit anti-goat IgG) were obtained from Molecular Probes. Additional reagents included Lipofectamine Plus reagent (Invitrogen), FuGENE-6 (Roche Applied Science), EZ-Link Sulfo-NHS-LC-Biotin (Pierce), (DAPT; Calbiochem), lactacystin, peptide aldehyde *N*-carbobenzoxyl-l-leucinyl-l-leucinyl-l-leucinal (MG-132), chloroquine (Calbiochem), and NH_4Cl (Calbiochem). The ECL-Plus kit was obtained from Amersham Biosciences. The β-amyloid 1–40 and 1–42 colorimetric enzyme-linked immunosorbent assay (ELISA) kit was purchased from BIOSOURCE International Inc.

cDNA Constructs—Expression vectors for all four human Numb isoforms have been described previously (28, 29). Full-length Numb, PTB deletion mutants of human Numb, or control expression plasmids were constructed as in-frame fusions downstream of the FLAG epitope. The plasmid for the dominant negative dynamin (dyn 1K44E tagged to hemagglutinin and enhanced green fluorescent protein) (30) was a kind gift from Dr. N. Bunnett (University of California, San Francisco, CA). The cDNA encoding dyn 1K44E was subcloned into the retroviral vector pBabe-puro (Addgene). The construct was transfected together with a plasmid encoding the vesicular stomatitis virus membrane glycoprotein envelope into 293T packaging cells (Clontech) using FuGENE-6, and the resulting virus-containing supernatant was collected at 48 and 72 h after transfection and used for transduction as described (31). Expression of exogenous dyn 1K44E was confirmed by immunoblotting.

Cell Lines and Transfections—PC12, HEK293, and SH-SY5Y cells were cultured under standard conditions in Dulbecco's modified Eagle's medium containing 10% fetal bovine serum (Invitrogen) and maintained at 37 °C in a 5% CO_2, 95% air atmosphere (32, 33). The PC12 cells stably expressing Numb variants have been described previously (28). SY5Y neuroblastoma cells stably transfected with a construct carrying the AD disease-linked double ("Swedish") mutation K595N/M596L in APP were obtained from Dr. W. Araki (National Institute of Neuroscience, Tokyo, Japan).

Treatments—Trophic factor withdrawal (TFW) was accomplished by washing the cells twice with phosphate-buffered

saline (PBS) and then maintaining them in Locke's buffer (29, 32). DAPT (2 μM) was used to inhibit γ-secretase activity. To inhibit proteasomes and lysosomes, cells were treated with proteasomal inhibitors MG-132 (5 μmol/liter) and *clasto*-lactacystin β-lactone (5 μmol/liter) or the lysosomal inhibitors chloroquine (100 μmol/liter) and NH_4Cl (50 mmol/liter) for various time periods. Inhibitors were resuspended either in DMSO or PBS. Controls were treated either with equivalent volumes of DMSO for the proteasome inhibitors or with equivalent volumes of PBS for chloroquine stimulations.

RNA Isolation and PCR—Total RNA from cells grown on 100-mm dishes was isolated with TRIzol (Invitrogen), and 2 μg of RNA was reverse transcribed with Superscript II reverse transcriptase and an oligo(dT) primer (32, 33). Quantitative real time PCR analyses of APP, Numb, and actin were performed using the following pairs of primers: rat APP, 5′-CCACTACCACAACTACCACTG-3′ (forward) and 5′-CCTCTCTTTGGCTTTCTGGAA-3′ (reverse); rat β-actin, 5′-TGTGATGGACTCCGGTGACGG-3′ (forward) and 5′-ACAGCTTCTCTTTGATGTCACGC-3′ (reverse); Rab5A, 5′-AACAAGACCCAACGGGCCAAATAC-3′ (forward) and 5′-ATACACAACTATGGCGGCTTGTGC-3′ (reverse); PTB-Numb, 5′-GGAAGTTCTTCAAAGGCTTCTTTG-3′ (forward) and PTB-Numb 5′-TTCATCCACAACTCTGAGTCCATC-3′ (reverse). The Numb primers were designed to flank the alternatively spliced insert in the PTB of the rat Numb cDNA sequence (accession number NM_133287).

SDS-PAGE and Western Blotting—Cells were harvested and lysed in buffer (100 mM Tris, pH 6.8, 1% SDS, 10 mM EDTA, 5 mM EGTA, 2 mM phenylmethylsulfonyl fluoride, 25 μg/ml leupeptin, 5 μg/ml pepstatin). The lysates were cleared by centrifugation at 13,000 $\times$ *g* for 20 min at 4 °C. The protein content of cell lysates was measured using BCA reagent (Pierce). Extracts containing 50 μg of protein were electrophoresed using Tris-HCl or 16.5% Tris-Tricine SDS-PAGE (Bio-Rad) under reducing conditions and immunoblotted onto nitrocellulose membranes (Bio-Rad). For immunodetection of blots, enhanced chemiluminescence (ECL; Amersham Biosciences) was applied. The optical band densities were quantified using NIH Image Analysis software.

Immunofluorescence Microscopy—Following experimental treatments, cells were fixed for 20 min in 4% paraformaldehyde in PBS at room temperature, permeabilized (or not) with 0.2% Triton X-100 in PBS, and incubated for 1 h in blocking solution (0.2% Triton X-100, 5% normal horse or goat serum in PBS) and then with primary antibody for 1 h in blocking solution at room temperature (32, 33). The cells were washed with PBS and finally incubated with 1 μg/ml Alexa Fluor 488 goat anti-rabbit IgG (1 μg/ml; Molecular Probes) in blocking solution at room temperature for 1 h. When double labeling was required, cell preparations were incubated with Alexa Fluor 488-conjugated anti-mouse IgG and rabbit Alexa Fluor 594-conjugated anti-goat IgG (1:200). Immunostained cells were observed with the appropriate filters on a Leica confocal laser-scanning microscope; average pixel intensity per cell was determined using software supplied by the manufacturer. Appropriate controls, such as secondary antibody alone, indicated a lack of nonspecific staining.

Measurements of sAPP Levels—For detection of sAPP, the media were collected from cultures of PC12 clones and centrifuged at 3,500 $\times$ *g* (10 min, 4 °C) to remove cell debris. The cleared supernatants were concentrated at least 20-fold by ultrafiltration. Cells were harvested, lysed, and prepared for protein determinations. Equal amounts of volumes of supernatants, standardized to lysate protein, were subjected to SDS-PAGE and immunoblotting analyses. All conditioned medium values were normalized to total protein lysates.

Aβ40/42 Sandwich ELISA—SH-SY5Y cells expressing the Swedish mutant APP were transfected with plasmids for the Numb variants or an empty pcDNA3 vector using Lipofectamine reagent according to the manufacturer's specifications. Conditioned media from transfected cells were collected 48 h after transfection, and protein inhibitors and 4-(2-aminoethyl)-benzenesulfonyl fluoride (Sigma) were added to prevent the degradation of Aβ. The concentration of Aβ40/42 in samples and standards was measured in duplicates using the β-amyloid 1–40 and 1–42 colorimetric ELISA kit according to the manufacturer's instructions (BIOSOURCE). Similar measurements of β-amyloid 1–40 were performed in PC12 cells subjected to TFW.

Measurements of Secretase Activity—The activity of APP secretases was determined using commercially available secretase kits (R&D Systems) according to the manufacturer's protocol. The method is based on the secretase-dependent cleavage of a secretase-specific peptide conjugated to the fluorescent reporter molecules EDANS and DABCYL, which results in the release of a fluorescent signal that can be detected using a fluorescence microplate reader (excitation at 355 nm/emission at 510 nm). The level of secretase enzymatic activity is proportional to the fluorimetric reaction.

Cell Surface Biotinylation—Confluent 10-cm dishes of each of the PC12 clones were washed three times with ice-cold PBS supplemented with 1 mM Ca^{2+} and 2 mM Mg^{2+} and incubated with 1 ml of biotin label (Pierce EZ-Link Sulfo-NHS-Biotin) at 2 mg/ml for 0.5 h on ice in the dark on a rotary mixer. The reaction was stopped by extensive washing with PBS and quenched with 50 mM glycine in PBS. Cell lysates were then immunoprecipitated with streptavidin-coated agarose. The precipitated biotinylated proteins were subjected to immunoblotting to analyze the content of APP and transferrin receptor.

Statistical Analyses—Statistical comparisons were made by using Student's *t* test and ANOVA with Scheffe *post hoc* tests for pairwise comparisons.

RESULTS

Expression of Numb Proteins Alters APP Metabolism in a Manner Dependent upon the PTB—To investigate the impact of Numb on APP metabolism, we stably overexpressed each of the four human Numb proteins in PC12 cells (28, 29). APP is physiologically processed by α-secretase or β-secretase, resulting in the shedding of nearly the entire ectodomain to yield large soluble APP derivatives (called sAPPα and sAPPβ, respectively) and generation of membrane-tethered APP-CTFs that include C83 and C99. The C99 is further cleaved by γ-secretase to release the ~4-kDa Aβ peptide and the APP intracellular domain. Stable expression of the SPTB-Numb proteins resulted

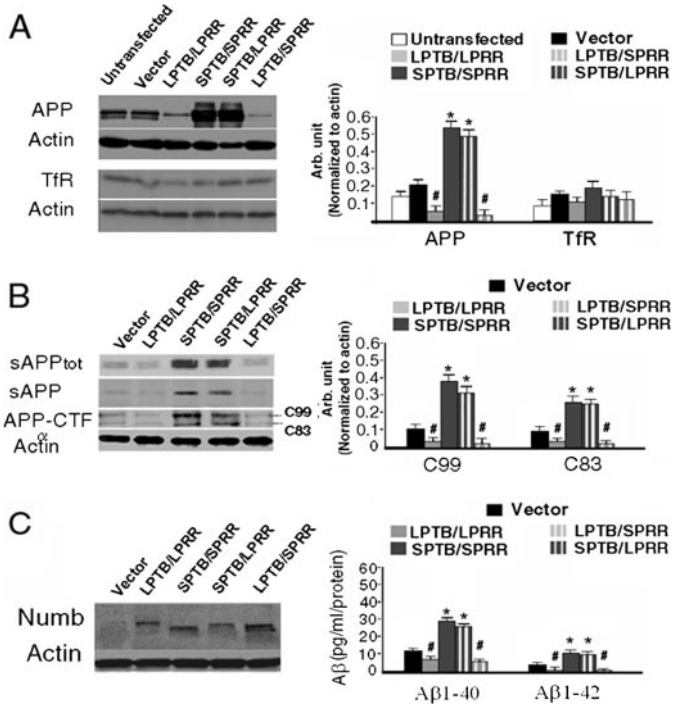

FIGURE 1. **Isoform specificity in the processing of APP and generation of Aβ by the Numb proteins.** *A*, effect of Numb proteins on the amounts of APP and TfR. *Left*, representative immunoblot showing total levels of APP and TfR protein in the indicated PC12 clones. Each *lane* was loaded with 50 μg of protein. The relative amounts of APP and TfR were normalized to those of actin. Densitometric analyses were performed on the immunoblots (*right*). The values in the *histogram* represent the mean ± S.D. $n = 3$; *, $p < 0.01$; #, $p < 0.05$ (ANOVA with Scheffe *post hoc* tests) relative to empty vector-transfected cells. *B*, effect of Numb proteins on the cleavage of APP. APP derivatives in the conditioned medium and in lysates of the indicated PC12 clones were quantified by Western blot followed by densitometric analyses. APP derivatives in conditioned culture medium were immunoprecipitated with an antibody to the amino-terminal domain of the APP protein (22C11), which precipitates both sAPPα and sAPPβ, and an antibody to Aβ (6E10; Signet), which recognizes sAPPα. Steady-state levels of membrane-associated APP derivatives, C99 and C83, were immunodetected with antibodies to the carboxyl-terminal domain of the APP protein. The β-actin signal represents the internal loading control. Densitometric analyses were performed on the immunoblots (*left*). The values in the *histogram* represent the mean ± S.D.; $n = 3$; *, $p < 0.01$; #, $p < 0.05$ (ANOVA with Scheffe *post hoc* tests) relative to vector-transfected control. Essentially similar results were obtained using two additional stable clones. *C*, effect of Numb proteins on the generation of Aβ peptides. SY5Y cells stably expressing the Swedish mutation of APP were transfected with plasmids encoding the FLAG-Numb proteins. Conditioned media were harvested and analyzed by a sandwich ELISA for specific quantitation of Aβ40 and Aβ42. Expression of FLAG-Numb proteins was detected by immunoblotting using an antibody to FLAG (*left*). The *histogram* shows the amounts of Aβ40 and Aβ42 in the indicated clones (*right*). The values represent the mean ± S.D.; $n = 3$; *, $p < 0.01$; #, $p < 0.05$ (ANOVA with Scheffe *post hoc* tests) relative to vector-transfected cells.

in a significant accumulation of intracellular APP (Fig. 1*A*) and increased secretion of sAPPα and sAPPβ in the conditioned media (Fig. 1*B*). By densitometric scanning of Western blots, the total amount of APP holoprotein in cells overexpressing the SPTB-Numb proteins was increased by 4–5-fold compared with parental control cells and by 8–10-fold compared with the LPTB-Numb clones.

The intracellular accumulation of APP holoprotein coincided with a significant increase in the amount of APP processing products. Both total sAPP and the amount of sAPPα immunoprecipitated from the conditioned media with anti-APP antibodies 22C11 and 6E10, respectively, were significantly higher in the SPTB-Numb clones. Steady-state levels of the α-secretase- and β-secretase-derived APP-CTFs, C83 and C99, respectively, were also increased in lysates, consistent with the ability of the SPTB-Numb proteins to promote nonamyloidogenic and amyloidogenic processing pathways (Fig. 1*B*). The opposite effect was observed in the clones expressing LPTB-Numb; steady state levels of APP holoprotein and APP processing products were markedly reduced relative to the parental clones. Only with long exposure times could the sAPP and APP-CTFs in the LPTB-Numb clones be detected. In contrast to APP, no change in the total levels of the transferrin receptor (TfR) (Fig. 1*A*) was found in the lysates, suggesting that the observed effects mediated by the Numb proteins were selective for APP. Collectively, the data indicate that the Numb proteins that differ in the PTB affect the processing of APP in a distinct and contrasting manner.

Expression of Numb Proteins Alters Aβ Generation in a Manner Dependent upon the PTB—Since the Numb proteins differentially affect APP cleavage and the generation of APP-CTFs, we reasoned that Numb should also influence the generation of Aβ. To test this notion, the cDNAs encoding FLAG-Numb variants were transfected into SY5Y cells expressing the Swedish mutant APP (Fig. 1*C*). Aβ40 and Aβ42 levels in the conditioned medium 48 h after transfection were determined using ELISA measurements. Consistent with the observed effects of Numb on the generation of APP-CTFs, we found that the LPTB-Numb proteins suppressed the production of Aβ40 and Aβ42 into the conditioned medium, whereas cells expressing the SPTB-Numb proteins generated elevated levels of Aβ40 (7.3 *versus* 28.5 pg/ml/protein) and Aβ42 (3.4 *versus* 13.2 pg/ml/protein) normalized to the total protein amount (Fig. 1*C*).

Expression of the Numb Proteins Does Not Affect the Level of APP Expression or the Proteolytic Activities of the APP-processing Secretases—One possible explanation for the effects of Numb on APP metabolism would be an alteration in the expression of APP. The presence of the Numb proteins had no significant effect on the levels of APP mRNA (Fig. 2*A*). We also considered the possibility that the Numb proteins might differentially alter the activities or the amounts of the APP-processing secretases. To investigate the influence of the Numb proteins on APP cleavages, we analyzed the proteolytic activities of α-, β-, and γ-secretases using commercially available secretase kits from R&D Systems. No significant difference in the proteolytic activities of these secretases was detected among the stable clones (Fig. 2*B*). In addition, we found that levels of BACE1 and of the γ-secretase components (presenilin-1, nicastrin, APH-1, and APH2) (34) were not altered by the expression of Numb (Fig. 2*C*), which further argued against a role of the Numb proteins in regulating the proteolytic activities of the secretases. Collectively, the data suggest that Numb proteins do not alter APP metabolism by regulating the expression of APP or the enzymatic activities of the secretases.

The Effects of Numb on APP Metabolism Are Dependent on Its Interaction with APP and the Internalization of APP—Next, we examined the interaction of the Numb proteins with APP to determine whether isoform-specific interactions could explain the contrasting effects of the Numb proteins on APP metabo-

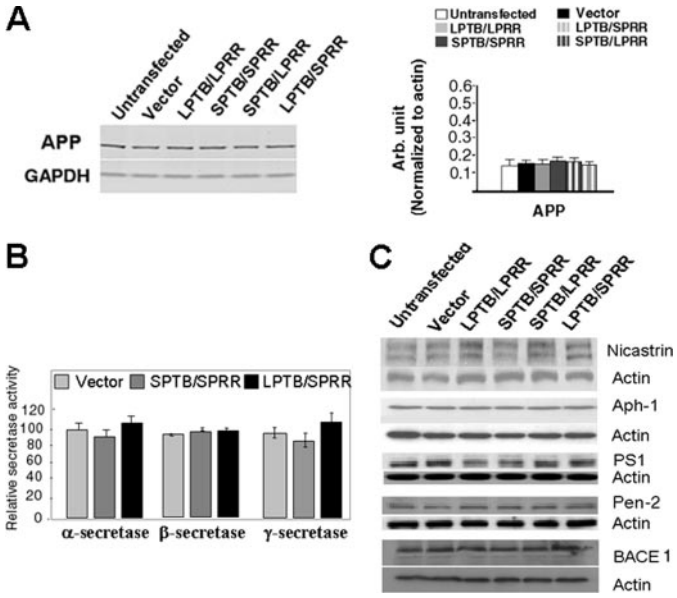

FIGURE 2. **Lack of isoform specificity on the expression of APP and the activities of the APP secretases.** *A*, expression of the Numb proteins did not alter the expression of APP. *Left*, semiquantitative real time PCR analysis of APP mRNA in the indicated PC12 clones. The glyceraldehyde-3-phosphate dehydrogenase signal represents the internal loading control. The values in the histogram are the mean ± S.D. of three independent measurements (*right*). Essentially similar results were obtained using two additional stably transfected clones. *B*, expression of the Numb proteins did not alter the activities of APP-processing secretases. The lysates were tested for secretase activities by the addition of secretase-specific peptide substrates conjugated to the reporter molecules EDANS and DABCYL (R&D Systems). Fluorescently labeled peptides were detected only upon cleavage by the respective secretases. After incubation at 37 °C for 2 h, reactions were transferred to a 96-well plate, and fluorescence was measured as described under "Experimental Procedures." The values expressed as arbitrary units of fluorescence (*AUF*) are the mean ± S.D. of at least three independent experiments. *C*, Numb proteins did not alter the protein level of β-secretase (*BACE1*) and of the components of the γ-secretase complex. Representative immunoblots show total levels of β-secretase, presenilin-1, nicastrin, Aph-1, and Pen-2 in the indicated clones. Each *lane* was loaded with 50 μg of protein. Blots were reprobed with an antibody against actin to confirm equal levels of protein loading among samples.

lism. Purified GST-fusion proteins of APP were mixed with lysates of 293 cells expressing a Numb protein isoform, and pull-down assays were performed. We found no differences in the ability of each Numb protein to interact with the APP protein (supplemental Fig. 1). Because the interaction of APP with Numb requires the YENPTY motif interacting with the PTB (26), we determined the effects of a Numb deletion mutant lacking the PTB (ΔPTB-Numb) on APP metabolism. Quantification of the Western blots (normalized to actin) revealed that APP metabolism was not altered in the presence of the ΔPTB-Numb protein (Fig. 3*A*), suggesting that the PTB is required for the Numb proteins to influence APP metabolism. To determine if the Numb proteins affect the proteolytic processing of APP by targeting APP along the endocytic rather than the secretory routes, we examined the effects of a dominant negative mutant dynamin (dyn 1K44E tagged to the hemagglutinin epitope and enhanced green fluorescent protein; a gift from N. Bunnett, University of California, San Francisco, CA) on the ability of each Numb protein to modulate APP metabolism. The GTPase dynamin is an important mediator of clathrin-dependent endocytosis (35) and is required for the internalization of many cell surface receptors including Notch (36) and APP (7). As expected, inhibition of endocytosis by mutant dynamin induced an elevation of APP holoprotein in all of the clones, including the LPTB-Numb clones (Fig. 3*B*). Total APP protein level in the SPTB-Numb and LPTB-Numb clones was not significantly different compared with those in the vector-transfected and parental clones. These results indicate that the Numb proteins differentially affect the processing of APP along the endocytic route.

Numb Proteins Influence the Endosomal Trafficking of APP—APP undergoes a retrograde transport back to the cell body wherein it is localized in Rab5a-positive early endosomes (37), late endosomes (8, 38), lysosomes (6), and the Golgi complex (8). To determine whether the Numb proteins affect the transport of APP to these intracellular compartments, we applied immunofluorescence microscopy to examine the subcellular localization of APP and Numb. Both of these proteins are colocalized on the plasma membrane and in vesicular structures in PC12 cells (Fig. 3*C*). Expression of the SPTB-Numb proteins resulted in a marked accumulation of APP in enlarged endosomes (Fig. 3*D*) that were positively labeled for Rab5a (Fig. 3*E*). Increased APP immunoreactivity was also detected in Rab11-labeled recycling endosomes (data not shown) but not in LAMP1-labeled lysosomal compartments of the SPTB-Numb clones (data not shown). The subcellular location of APP was similar to that of Numb, suggesting that Numb interacts with APP in the early endocytic compartments. By contrast, APP was only faintly detected in the Rab5-labeled (Fig. 3*E*), Rab11-labeled, and LAMP1-labeled compartments (data not shown) in LPTB-Numb clones. Collectively, these data suggest that the PTB of Numb determines the processing fates of APP by regulating its endosomal sorting and trafficking to distinct compartments.

Effect of the Numb Proteins on the Endosomal Sorting of APP to the Recycling Pathway—Despite the accumulation of APP in the enlarged early endosomes (Fig. 3*D*), SPTB-Numb clones exhibited increased release of sAPPα and generation of C83, suggesting that APP may be preferentially sorted from the early endosomes back to the cell surface, where APP is cleaved by α-secretase. To evaluate the amount of APP localized on the cell surface, we performed cell membrane staining for APP on ice without permeabilization. Only a small fraction of APP was detected at the cell surface of parental cells not permeabilized prior to antibody incubation (Fig. 4*A*), consistent with a previous report (5). The fraction of cell surface-bound APP was markedly higher in the SPTB-Numb clones. As expected, this fraction was significantly lower in the LPTB-Numb clones compared with parental cells. As another measure of surface APP protein level, proteins on the cell surface were biotinylated with a cell-impermeant cross-linker, collected with neutravidin-coupled beads, and subjected to immunoblotting. As expected, the level of biotinylated plasma membrane-bound APP was significantly higher in SPTB-Numb clones (Fig. 4*C*). By densitometric scanning of Western blots, the amount of cell surface-localized APP relative to TfR was approximately 5-fold higher in cells overexpressing SPTB-Numb compared with vector-transfected cells (Fig. 4*C*). None of the biotinylated fractions contained actin consistent with the labeling of only cell surface-bound proteins (Fig. 4*B*).

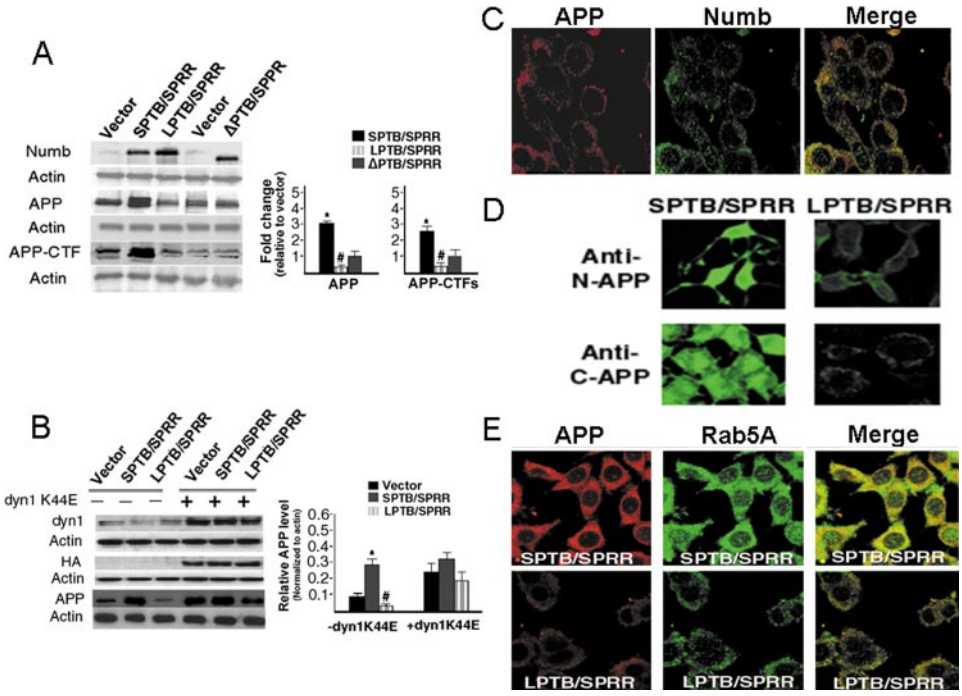

FIGURE 3. **Isoform specificity of Numb effects on APP metabolism is dependent on the interaction of the Numb proteins with APP and its subsequent internalization.** *A*, expression of a Numb protein lacking the PTB (ΔPTB-Numb) did not alter APP metabolism. *Left*, representative immunoblot showing total levels of APP holoprotein in the indicated PC12 clones. Each *lane* was loaded with 50 μg of protein. APP was quantified by Western blot with an antibody to the amino-terminal domain of the APP protein, followed by densitometric analyses (*right*). The relative amounts of APP were normalized to those of actin. *B*, inhibition of endocytosis by overexpression of mutant dyn 1K44E abolished the effects of the Numb proteins on APP metabolism. Twenty-four hours after transduction, cell lysates were analyzed by immunoblotting, followed by densitometry (*right*). A representative immunoblot shows total levels of APP in the indicated PC12 clones. Overexpression of the dyn 1K44E was confirmed using antibodies raised to dyn 1 and to the hemagglutinin tag. The β-actin signal represents the internal loading control. The values in the *histogram* represent the mean ± S.D. $n = 3$; *, $p < 0.01$; #, $p < 0.05$ (ANOVA with Scheffe *post hoc* tests) relative to vector-transfected cells. *C*, localization of APP and Numb in PC12 cells by confocal immunofluorescence microscopy. Following fixation and permeabilization, rabbit anti-Numb- and goat anti-rabbit-conjugated fluorescein isothiocyanate, mouse anti-APP (22C11), and goat anti-mouse-conjugated CY3 secondary antibody were used to detect Numb and APP protein, respectively. The *right panel* shows the merged image of APP and Numb. *D*, intracellular accumulation of APP and membrane-associated APP derivatives in a SPTB-Numb (*left*) and LPTB-Numb clone (*right*). Following fixation and permeabilization, APP was detected with antibodies to the amino- and carboxyl-terminal domains of the APP protein. *E*, localization of APP to endocytic compartments by confocal immunofluorescence microscopy. Following fixation and permeabilization, rabbit anti-Rab5A and goat anti-rabbit conjugated fluorescein isothiocyanate were used to detect the early endosomes (*green signal*), and mouse anti-APP (22C11) and goat anti-mouse-conjugated CY3 secondary antibody were used to detect APP protein (*red signal*). The *right side* of each *image* shows the *merged image* of APP and Rab5, depicting early endosomes. The *images* are representative of those obtained from at least three stably transfected clones.

Effect of the Numb Proteins on the Endosomal Sorting of APP to the Degradative Pathway—To further establish that altered subcellular localization of APP is responsible for the differences in its processing fates in the Numb clones, we treated PC12 clones with chloroquine, a weak base known to disrupt lysosomal function by blocking organellar acidification (42). Treatment with chloroquine (100 μM) for up to 6 h (Fig. 5*A*) and longer (data not shown) had no marked effects on the levels of APP (Fig. 5*A*) and APP-CTF derivatives (data not shown) in SPTB-Numb clones. Similar results were obtained in the presence of ammonium chloride (NH_4Cl; 50 mmol/liter), confirming that the available pools of APP in the SPTB-Numb cells were absent from the lysosomes (Fig. 5*B*). By contrast, levels of APP protein (Fig. 5*A*) and APP-CTF derivatives (data not shown) in LPTB-Numb clones were significantly increased following chloroquine treatment in comparison with vector-transfected cells, ruling out the possibility that chloroquine at the concentration of 100 μM was too low to induce APP accumulation in the SPTB-Numb clone (Fig. 5*A*). The same dose of chloroquine also caused marked accumulation of APP and APP-CTFs in SH-SY5Y cells stably transfected with the empty vector or with the Swedish mutant APP (Fig. 5*C*). The effect of lysosomal inhibitors on APP protein levels was dose-dependent (data not shown). Control incubation of PC12 clones with PBS resulted in unchanged levels of APP (data not shown). To determine that the chloroquine-induced increase in APP holoprotein was not related to an effect of Numb on the synthesis of APP, we treated cells with the protein synthesis blocker cycloheximide (10 μg/ml) in combination with chloroquine. Treatment with cycloheximide for 6 h did not prevent the chloroquine-induced increase in APP holoprotein (data not shown).

In contrast to lysosomal inhibitors, we found that treatment with the γ-secretase inhibitor DAPT markedly enhanced steady state levels of APP and APP-CTFs in the SPTB-Numb clone (Fig. 5*D*). The APP-CTFs were only weakly detected in the vector cells but became clearly visible, as in the untreated SPTB-Numb clones, after treatment with DAPT, which halted the cleavage of membrane-associated APP-CTFs. The effect of DAPT on APP protein levels was dose-dependent (data not

To determine whether vesicle recycling contributed to the increased cell surface expression of APP in the SPTB-Numb clone, we assessed the impact of a blockade in the endosome recycling pathway. Preincubation with monesin, an established inhibitor of the recycling pathway that does not interfere with the initial endocytosis of surface receptor proteins (43), significantly depleted cell surface APP expression, as assessed by surface biotinylation followed by immunoblotting of the isolated biotinylated fraction (Fig. 4*D*). The surface receptor-depleting effect of monesin on TfR was only slightly reduced in the absence of ligand (Fig. 4*D*), suggesting that the recycling pathway of APP may be mechanistically distinct from that of TfR. Quantification of the immunoblots revealed that the changes in the ratio of APP to TfR after treatment with monesin was significantly greater in the SPTB-Numb clone compared with the vector-transfected cells (Fig. 4*E*).

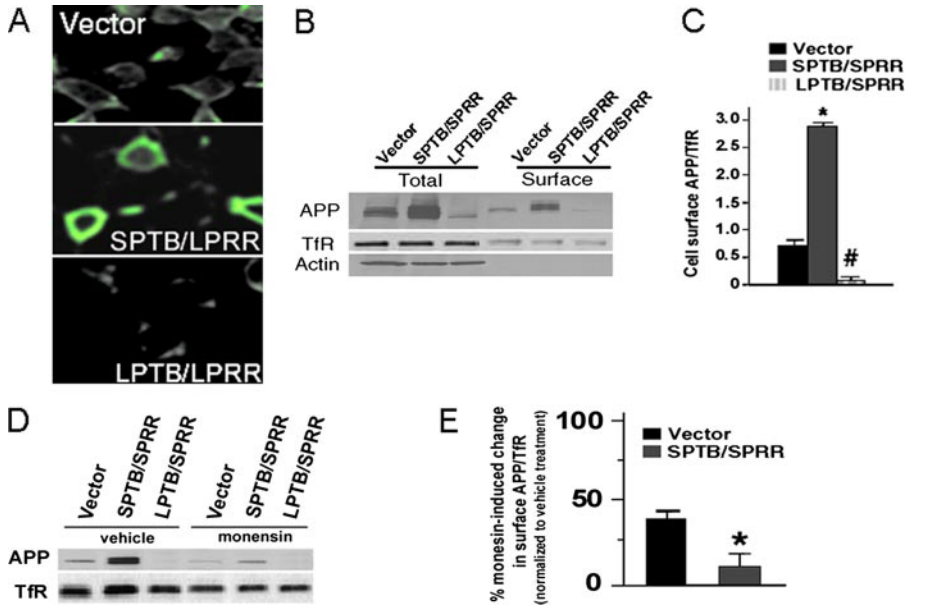

FIGURE 4. **Effect of the Numb proteins on the sorting of APP to the recycling pathway.** *A*, the Numb proteins differentially alter the amount of cell surface APP. Immunostaining of cell surface APP with an antibody to the amino-terminal end of APP is shown. In nonpermeabilized cells (without Triton X-100), significantly more APP is detected on the surface of a SPTB-Numb clone compared with a LPTB-Numb clone or a clone transfected with empty vector. *B*, detection of cell surface APP by biotinylation. Cells were surface-biotinylated, lysed, and incubated with streptavidin-agarose beads. Biotinylated proteins were immunoblotted with antibodies to APP and TfR. *C*, quantitative data showing the ratio of cell surface APP and TfR in the indicated clones. Values are the mean ± S.D. of at least three independent experiments. *, $p < 0.01$; #, $p < 0.05$ (ANOVA with Scheffe *post hoc* tests) relative to vector-transfected cells. *D*, recycling blockade depletes cell surface APP protein level. The indicated clones were pretreated with monensin for 60 min at 37 °C in Dulbecco's modified Eagle's medium/bovine serum albumin and incubated in Dulbecco's modified Eagle's medium/bovine serum albumin for 60 min afterward. Cells were then surface-biotinylated using a membrane-impermeable cross-linker and immunoprecipitated with streptavidin beads. Precipitates were subjected to SDS-PAGE, and blots were probed with antibodies to APP and TfR. *E*, quantitative data showing the changes in the ratio of cell surface APP and TfR in the vector-transfected and a SPTB-Numb clone after monesin treatment. Values are plotted as percentage of untreated control (vehicle) and are the mean ± S.D. of at least three independent experiments. *, $p < 0.05$ (Student's *t* test) relative to vector-transfected cells.

shown). In contrast, DAPT failed to elevate levels of APP-CTFs in the LPTB-Numb clones. Collectively, our data indicate that the Numb proteins target APP to endocytic compartments with distinct APP processing outcomes.

The Proteasome-mediated Degradative Pathway Is Not Involved in the Regulation of APP Metabolism by the Numb Proteins—Considerable evidence indicates that Numb antagonizes Notch signaling transduction by activating the endocytic uptake and degradation of the Notch protein via the proteasomal degradation pathway (21, 40). Because of the striking similarities in the proteolytic processing of Notch and APP, we hypothesized that the LPTB-Numb proteins may reduce APP protein levels by facilitating proteasomal-mediated degradation of APP. To test this hypothesis, we treated the stable clones with lactacystin, which inhibits proteasomal degradation of proteins by specifically targeting the 20 S proteasome, without interfering with lysosomal protein degradation (41). Treatment with lactacystin did not result in significant changes in APP protein levels and did not impact the generation of APP metabolites in any of the clones tested (Fig. 5*E*), suggesting that the differential effects of the Numb proteins on APP metabolism did not involve the ubiquitin-proteasome protein degradation pathway. Higher concentrations of lactacystin did not significantly induce APP accumulation, although the dose of 10 μM was sufficient to induce enrichment of ubiquitinated protein species in general, as shown in Western blot analysis conducted with an antibody to ubiquitin (data not shown). Collectively, the data indicate that the drastic reduction in APP protein level in the LPTB-Numb clones was not due to Numb-mediated targeting of APP for proteasome-dependent degradation.

Expression of Numb Proteins Alters the Levels of the Rab Family of Endocytic Regulators—Recent studies have demonstrated the involvement of GTP-binding proteins of the Rab family in the trafficking and processing of APP (44, 45). Rab proteins are localized in both discrete organelles and vesicles, where they play key roles in protein trafficking between compartments along the secretory and endocytic routes. To determine whether the differential endosomal sorting of APP resulted from the altered expression of Rab proteins, we measured protein levels of Rab4, Rab5A, Rab7, and Rab11. Rab5A is a small GTPase localized on early endosomes and controls endosome fusion along the endocytic pathway. Rab4A and Rab11 are regulators of the recycling endosomes (44, 45). Protein levels of Rab4A, Rab5A, and Rab11 were significantly increased in the SPTB-Numb clones relative to control cells (Fig. 6, *A* and *B*). By contrast, levels of Rab5A and Rab11 were decreased in the LPTB-Numb clones relative to control cells (Fig. 6, *A* and *B*). Levels of Rab7, a regulator of fusion events in the late endocytic pathway, and of LAMP-1 (lysosome-associated membrane protein-1) were not different among the stable clones (Fig. 6, A and *B*). The changes in the level of the Rab5A protein were not attributable to altered expression, since its mRNA level was not significantly different in the stably transfected Numb clones (Fig. 6*C*).

Stress Induces the Selective Up-regulation of SPTB-Numb Transcripts—It has been previously reported that alternative splicing of Numb primary transcripts is developmentally regulated (45, 46). To determine whether the balance of the alternative spliced variants of Numb might be disrupted in cells that were stimulated by apoptosis-inducing agents, we designed oligonucleotide primers that bind to the flanking sequences of the insertion in the PTB (Fig. 7*A*). The expected sizes of the amplified PCR products for the SPTB- and LPTB-Numb transcripts were 114 and 147 base pairs, respectively. The level of LPTB-Numb mRNA that is predominantly expressed under basal condition decreased rapidly upon TFW, an insult that has previously been shown to alter Numb expression (29), whereas that of SPTB-Numb accumulated concomitantly in stressed cells

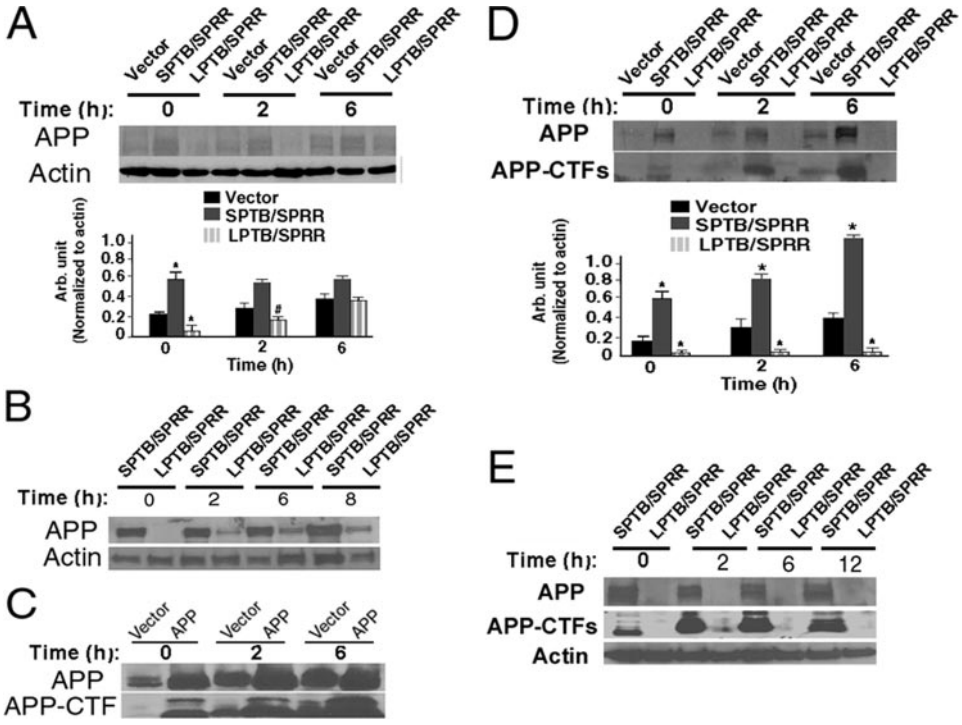

FIGURE 5. **Effect of the Numb proteins on the sorting of APP to the degradative pathway.** *A*, time course of the accumulation of APP and APP-CTFs in LPTB-Numb but not SPTB-Numb clones after treatment with a lysosomal inhibitor. The indicated stable PC12 clones were treated with choroquine (100 μM) for 0, 2, and 6 h. Equal amounts of cellular lysates were separated by 16.5% Tris-Tricine SDS-PAGE and immunoblotted with an antibody to the carboxyl terminus of APP. β-Actin was used as the internal loading control. Densitometric analyses were performed on the immunoblots (*bottom*). The values in the histogram are the mean ± S.D. of three independent measurements. *, $p < 0.01$; #, $p < 0.05$ (ANOVA with Scheffe *post hoc* tests) relative to vector-transfected cells. Similar results were obtained using two additional stably transfected Numb clones. *B*, time course of the accumulation of APP in LPTB-Numb but not SPTB-Numb clones upon treatment with NH_4Cl. The indicated clones were treated with NH_4Cl (50 μM) for 0, 2, 6, and 8 h and processed for immunoblotting using an antibody to the carboxyl-terminal of APP. *C*, time course of the accumulation of APP and APP-CTFs in SH-SY5Y cells overexpressing the empty vector (*Vector*) or a vector encoding the Swedish mutant APP (*APP*) upon chloroquine treatment. The indicated SY-SY5Y clones were treated with choroquine (100 μM) for 0, 2, and 6 h. Each *lane* was loaded with 50 μg of protein. β-Actin was used as the internal loading control. *D*, time course of the accumulation of APP in the SPTB-Numb but not LPTB-Numb clones after treatment with the γ-secretase inhibitor DAPT. The indicated clones were treated for 0, 2, 6, and 12 h with 10 μM DAPT. Each *lane* was loaded with 50 μg of protein. β-Actin was used as the internal loading control. Densitometric analyses were performed on the immunoblots (*bottom*). Values are the means ± S.D. of three independent measurements. *, $p < 0.01$ (ANOVA with Scheffe *post hoc* tests) relative to empty vector-transfected cells. *E*, inhibition of the proteasomes failed to affect the regulation of APP metabolism by the Numb proteins. Time course of the levels of APP and APP-CTFs in the indicated clones after treatment with 10 μM lactacystin. Equal amounts of protein from each sample were immunoblotted to detect APP and APP-CTFs. Each *lane* was loaded with 50 μg of protein and verified with an antibody to actin. Essentially similar results were obtained using two additional stably transfected Numb clones.

endocytosis and endosome recycling. Aβ immunoreactivity is evident in these populations of enlarged endosomes prior to Aβ deposition indicating their potential importance for Aβ formation in early AD brain. Much attention has focused on the mechanisms that regulate the trafficking of APP to endosomes. In this study, we have uncovered a novel function for the Numb adapter proteins as a regulator of endocytic trafficking of APP. Most surprisingly, we found that the Numb proteins that differ in the PTB, but not in the PRR domain, have opposite effects on the transport and processing of APP. The expression of SPTB-Numb proteins resulted in a significant accumulation and persistence of APP holoprotein in the early endosomes and increased Aβ secretion. By contrast, expression of LPTB-Numb proteins significantly decreased the accumulation of APP and inhibits Aβ secretion. The reduction in Aβ secretion was not the result of either the decreased expression of APP or a significant reduction in the activities of the APP processing secretases. Furthermore, we demonstrated that all the Numb isoforms were capable of interacting with the APP holoprotein, as reported by a previous study (26). The APP-lowering effect was related to the trafficking role of the LPTB-Numb proteins along the endocytic rather than the secretory pathway as treatment with lysosomal inhibitors was able to restore endogenous APP holoprotein to the steady state level found in vector-transfected cells. It is conceivable that LPTB-Numb but not SPTB-Numb proteins facilitate the delivery of APP to the lysosomes for degradation by acidic hydrolases. Taken together, these results indicate that APP trafficking differs strikingly in the clones stably expressing the Numb proteins and raise the intriguing possibility that alternative splicing of Numb could alter the trafficking of APP and, concomitantly, its processing fate.

(Figs. 7, *B* and *C*). Protein but not mRNA levels of APP were also increased in PC12 cells subjected to TFW (Fig. 7*D*). TFW markedly increased the production of Aβ 1–40 (Fig. 7*E*). Collectively, these data suggest that cellular stress could induce the selective up-regulation of SPTB-Numb proteins, which precedes the accumulation of APP protein. The stress-induced changes in Numb isoform expression and the subsequent Numb isoform-dependent effect on APP trafficking and processing are schematically summarized in Fig. 8.

DISCUSSION

Alterations in the endosomal-lysosomal system are believed to occur early in the disease process in AD, and may precede the formation of plaques and tangle-associated neuropathology in susceptible neuron populations. Endosome enlargement occurs early in sporadic AD, and is associated with increased

Numb was discovered as an intracellular Notch antagonist (17, 19). Considerable evidence over the past years has indicated that Numb antagonizes Notch1 signaling by inducing Notch1 ubiquitination and endocytic degradation of NICD (21, 41). Genetic and biochemical evidence in invertebrates has suggested that proteasomal degradation of Notch may be required for the cessation of Notch signaling (21, 41). Numb has been shown to recruit the E3 ubiquitin ligase to facilitate Notch

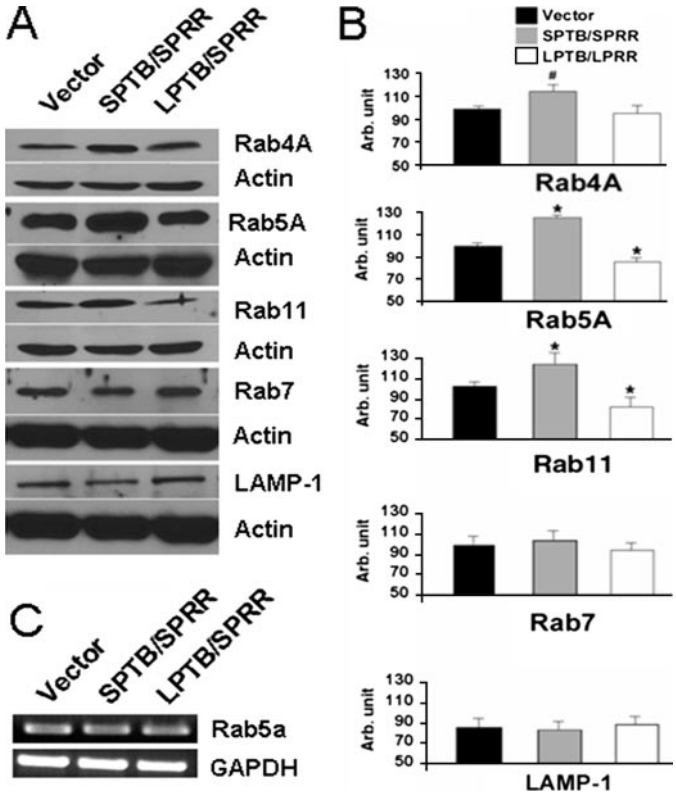

FIGURE 6. **Effect of the Numb proteins on the levels of small Rab GTPases.** *A*, representative immunoblots showing total amounts of Rab4A, Rab5A, Rab7, Rab11, and LAMP1 in the indicated clones. Each *lane* was loaded with 50 μg of protein and verified with an antibody to actin. *B*, densitometric analyses were performed on the immunoblots shown in *A*. The values in the histogram are the mean ± S.D. of three independent measurements. *, $p < 0.01$; #, $p < 0.05$ (ANOVA with Scheffe *post hoc* tests). *C*, semiquantitative real time PCR analysis of Rab5A mRNA in the indicated PC12 clones. The glyceraldehyde-3-phosphate dehydrogenase signal represents the internal loading control.

receptor ubiquitination (21). Several E3 ubiquitin ligases, such as LNX, Itch, Siah1, and Mdm2, have been shown to associate with Numb (21, 47–49). To exclude the possibility that LPTB-Numb targets APP for proteasomal degradation, we found that proteasomal inhibition had no marked effect on the accumulation of APP in the stable clones examined, suggesting that Numb did not target APP for proteasomal degradation.

The PTB is a protein-protein interaction motif that has been identified in a diverse group of proteins, of which only a subset is linked to tyrosine kinase-mediated signaling (50). Structure-function analyses indicated that the Numb PTB can bind to multiple conformationally distinct peptide ligands in a phosphotyrosine-independent manner (51–53). The PTB of Numb has been shown to interact with diverse proteins that determine its subcellular localization (54) and protein stability (55). The PTB of Numb mediates the interaction with the E3 ubiquitin ligases responsible for the ubiquitination of its bound substrates, such as Notch and Gli (17, 21). Hence, the presence or absence of the insertion within the PTB could impact the interaction of the Numb proteins with E3 ligases and the targeted substrates (17, 56). We found that the insert in the PTB did not affect the ability of the Numb proteins to interact with APP, in accord with a previous study showing that APP was found in complex with all four mammalian Numb isoforms in cortical lysates (26). Furthermore, the insert of the PTB did not alter the subcellular localization of the Numb proteins (28, 29), suggesting that the differential effects of the Numb proteins on APP metabolism could not be attributed to the preferential targeting of LPTB-Numb proteins to membrane-bound APP. The present study showed that Numb can bind directly to the YENPTY motif in the cytoplasmic domain of APP (supplemental Fig. 1), an interaction that is not only required for the internalization of cell surface APP but also for its subsequent transport and processing fate (57).

The accumulation of APP holoprotein did not correlate with a reduction of Aβ secretion, which supports the contention that the Numb proteins influence the trafficking of endogenous APP along endocytic rather than secretory routes. Additional data showed that inhibition of endocytosis by overexpression of a dominant-negative dynamin negates the observed effects of the Numb proteins on APP metabolism. Furthermore, treatment of the Numb clones with brefeldin A to inhibit the transport of proteins from the endoplasmic reticulum to the Golgi did not show any effect on APP accumulation (data not shown), whereas lysosomal inhibitors restored steady state levels of APP in the LPTB-Numb clones (Fig. 5).

The reduced sensitivity of the SPTB-Numb clones to inhibition of lysosomal degradation suggests that these Numb proteins may interfere with the transport of APP to the degradative pathway. Alternatively, we cannot rule out the possibility that these Numb proteins play an active role in recycling internalized APP back to the cell surface. This notion is consistent with the increased amounts of released sAPPα and intracellular C83 generated by α-secretase cleavage, which occurs mainly at the cell surface. Since dissociation of protein-protein complexes favors the recycling pathway, it remains to be elucidated whether the interaction of the Numb proteins and APP results in conformational changes that are differentially resistant to decreasing pH values within the endosomal pathway. Regardless of the underlying molecular mechanisms, our data suggest that the Numb proteins differentially alter the endocytic trafficking of APP by regulating the endosomal sorting of this protein either to the degradative or recycling pathway. It will be interesting to examine whether the Numb proteins differentially affect the trafficking of other receptors with the conserved YENPTY motif, such as TrkA, a tyrosine kinase receptor whose protein level and responsiveness to nerve growth factor were shown to be differentially affected by the Numb proteins (28).

Whether the Numb proteins are directly involved in the active transport of APP remains to be elucidated. Intracellular trafficking through the endocytic and recycling pathway is regulated by the small GTPase Rab proteins, whose altered expression and activity has been linked to altered APP metabolism (9, 10, 44). Rab5A up-regulation is associated with enlarged early endosomes and intracellular accumulation of APP (9). Altered Rab5A activity is responsible for the early abnormalities of the neuronal endocytic pathway that are directly related to a rise in Aβ levels in the brains of AD patients (9, 10). Previous studies demonstrated that Numb interacts with Arf6 and EHD4 (58), proteins that have been associated with the recycling of plasma membrane proteins internalized by clathrin-dependent and clathrin-independent endocytic routes (59). Impairments in

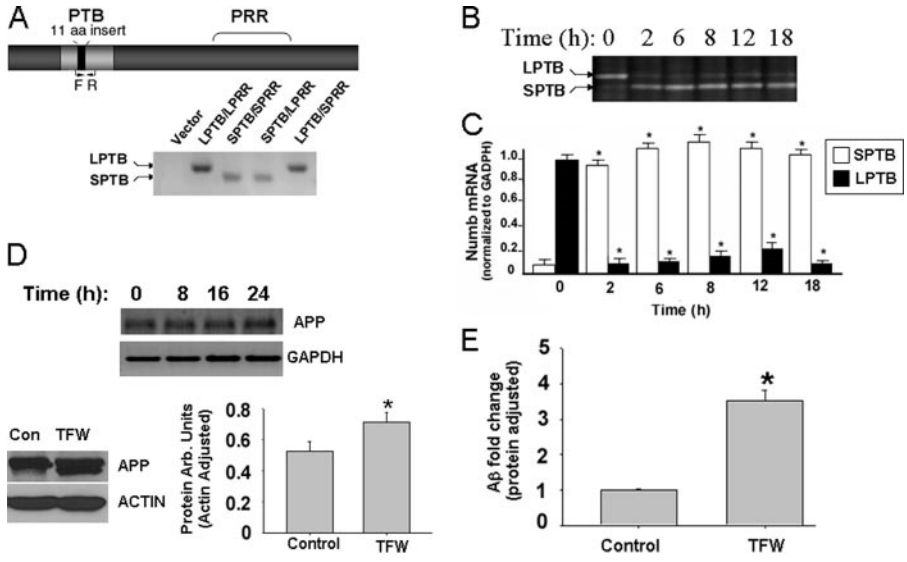

FIGURE 7. **Detection of alternatively spliced Numb transcripts under normal and stressed conditions.** *A*, domain structure of the Numb protein. The 11-amino acid insertion in the PTB is indicated in *black*. The forward (*F*) and reverse (*R*) primers were designed to amplify a region flanking the PTB insertion. The specificity of the primer set was confirmed by performing PCR using an empty plasmid (pCDNA3.1) or plasmids containing each of the four Numb isoforms. The expected sizes of PCR fragments were 114 and 147 base pairs for the SPTB- and LPTB-Numb transcripts, respectively. *B*, time course of SPTB-Numb and LPTB-Numb mRNA levels in PC12 cells subjected to TFW. *C*, densitometric analyses were performed on the data shown *B*. The values in the *histogram* are the mean ± S.D. of three independent measurements. *, $p <$ 0.01 (Student's *t* test) relative to untreated control PC12 cells. *D*, effect of stress-induced Numb isoform change on APP processing. *Top*, semiquantitative real time PCR analysis of APP mRNA levels in PC12 before and after TFW for the indicated times. The glyceraldehyde-3-phosphate dehydrogenase signal represents the internal loading control. *Bottom*, representative immunoblots showing total levels of APP in PC12 cells left untreated (*Con*) or subjected to TFW for 24 h. Each lane was loaded with 50 μg of protein. β-Actin was used as the internal loading control. Densitometric analyses were performed on the immunoblots. The values in the *histogram* represent the mean ± S.D. of three independent measurements. *, $p < 0.05$ (Student's *t* test) relative to nontreated cells. *E*, effect of stress-induced Numb isoform change on the generation of Aβ. PC12 cells were left untreated (*Con*) or subjected to TFW for 24 h. Conditioned media were harvested and analyzed by a sandwich ELISA for specific quantitation of Aβ40. The *histogram* shows the relative amounts of Aβ40. The values represent the mean ± S.D.; $n = 3$; *, $p < 0.01$ (Student's *t* test) relative to nontreated control cells.

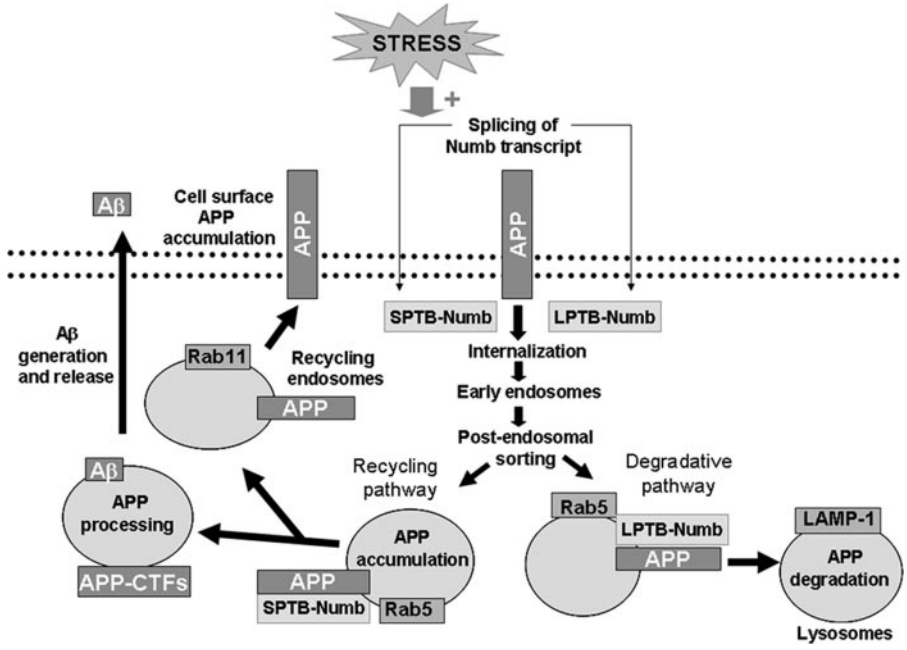

FIGURE 8. **Summary diagram showing the effects of the alternatively spliced Numb isoforms on the trafficking and processing of APP.**

the sorting pathway could also account for the intraneuronal Aβ accumulation in the brains of APP mutant transgenic mice and human AD patients (60). We found that level of Rab5A protein but not mRNA was elevated in the SPTB-Numb clones, suggesting that altered Rab5A function in part correlates specifically with altered trafficking of APP. The mechanism(s) whereby expression of SPTB-Numb increases protein level of Rab5A but not mRNA remains to be established.

At present, the factors that regulate the alternative splicing of the primary Numb transcript are not known. It has been shown that the four Numb isoforms are temporally regulated and implement distinct developmental functions (45, 46). Ectopic expression of Numb isoforms lacking the PRR insertion promotes differentiation, whereas those isoforms with the insertion direct proliferation. Indeed, the expression of LPRR-Numb isoforms that promote proliferation peaks during the expansion of the neural progenitor pool but is down-regulated during the course of neuronal development (45, 46). The expression pattern of the Numb proteins also varies dramatically between different tissues and cultured cell lines, suggesting that Numb isoforms may have different functions in different cell types. Our previous study demonstrated that Numb protein levels increased in Aβ-laden brain regions of a mouse model of AD (29). In this study, we found for the first time that pathophysiological conditions can up-regulate the expression of SPTB-Numb at the expense of LPTB-Numb. This finding raises the intriguing possibility that altered Numb expression is an early pathologic event that may be responsible for increased Aβ production in patients with AD.

Although the exact function of APP is still not resolved, experimental evidence suggests several activities, including synaptogenesis, neurite outgrowth, and cell survival in neurons (1). All of these activities

may potentially be affected by the presence of Numb proteins determining the processing fates of APP. Of particular note is that overexpression of SPTB-Numb in PC12 cells enhanced neurite outgrowth (28) and increased vulnerability to apoptotic stimuli by a mechanism dependent on the dysregulation of intracellular Ca^{2+} homeostasis (28, 29). How Numb modulates intracellular Ca^{2+} homeostasis remains to be elucidated. The disruption in Ca^{2+} signaling may be linked to altered APP metabolism (1, 39), suggesting the involvement of altered Numb function or expression in the genesis of the AD phenotype. Hence, perturbation of Numb expression may have important implications for AD pathogenesis.

REFERENCES

1. Mattson, M. P. (1997) *Physiol. Rev.* **77,** 1081–1132
2. Selkoe, D. J. (2001) *Physiol. Rev.* **81,** 741–766
3. Gandy, S., Caporaso, G., Buxbaum, J., Frangione, B., and Greengard, P. (1994) *Neurobiol. Aging* **15,** 253–256
4. Selkoe, D. J., Yamazaki, T., Citron, M., Podlisny, M. B., Koo, E. H., Teplow, D. B., and Haass, C. (1996) *Ann. N. Y. Acad. Sci.* **777,** 57–64
5. Weidemann, A., König, G., Bunke, D., Fischer, P., Salbaum, J. M., Masters, C. L., and Beyreuther, K. (1989) *Cell* **57,** 115–126
6. Haass, C., Koo, E. H., Mellon, A., Hung, A. Y., and Selkoe, D. J. (1992) *Nature* **357,** 500–503
7. Carey, R. M., Balcz, B. A., Lopez-Coviella, I., and Slack, B. E. (2005) *BMC Cell Biol.* **6,** 30–35
8. Koo, E. H., and Squazzo, S. L. (1994) *J. Biol. Chem.* **269,** 17386–17389
9. Grbovic, O. M., Mathews, P. M., Jiang, Y., Schmidt, S. D., Dinakar, R., Summers-Terio, N. B., Ceresa, B. P., Nixon, R. A., and Cataldo, A. M. (2003) *J. Biol. Chem.* **278,** 31261–31268
10. Cataldo, A. M., Barnett, J. L., Pieroni, C., and Nixon, R. A. (1997) *J. Neurosci.* **17,** 6142–6151
11. Uemura, T., Shepherd, S., Ackerman, L., Jan, L. Y., and Jan, Y. N. (1989) *Cell* **58,** 349–360
12. Rhyu, S., Jan, L. Y., and Jan, Y. N. (1994) *Cell* **76,** 477–491
13. Verdi, J. M., Schmandt, R., Bashirullah, A., Jacob, S., Salvino, R., Craig, C. G., Program, A. E., Lipshitz, H. D., and McGlade, C. J. (1996) *Curr. Biol.* **6,** 1134–1145
14. Dho, S. E., French, M. B., Woods, S. A., and McGlade, C. J. (1999) *J. Biol. Chem.* **274,** 33097–33104
15. Santolini, E., Puri, C., Salcini, A. E., Gagliani, M. C., Pelicci, P. G., Tacchetti, C., and Di Fiore, P. P. (2000) *J. Cell Biol.* **151,** 1345–1352
16. Berdnik, D., Torok, T., Gonzalez-Gaitan, M., and Knoblich, J. A. (2002) *Dev. Cell* **3,** 221–231
17. Guo, M., Jan, L. Y., and Jan, Y. N. (1996) *Neuron* **17,** 27–41
18. Huang, E. J., Li, H., Tang, A. A., Wiggins, A. K., Neve, R. L., Zhong, W., Jan, L. Y., and Jan, Y. N. (2005) *Genes Dev.* **19,** 138–151
19. Wakamatsu, Y., Maynard, T. M., Jones, S. U., and Weston, J. A. (1999) *Neuron* **23,** 71–81
20. Mumm, J. S., and Kopan, R. (2000) *Dev. Biol.* **228,** 151–165
21. McGill, M. A., and McGlade, C. J. (2003) *J. Biol. Chem.* **278,** 23196–23203
22. Frise, E., Knoblich, J. A., Younger-Shepherd, S., Jan, L. Y., and Jan, Y. N. (1996) *Proc. Natl. Acad. Sci. U. S. A.* **93,** 11925–11932
23. Spana, E. P., and Doe, C. Q. (1996) *Neuron* **17,** 21–26
24. Nishimura, T., Fukata, Y., Kato, K., Yamaguchi, T., Matsuura, Y., Kamiguchi, H., and Kaibuchi, K. (2003) *Nat. Cell Biol.* **5,** 819–826
25. Nishimura, T., and Kaibuchi, K. (2007) *Dev. Cell* **13,** 15–28
26. Roncarati, R., Sestan, N., Scheinfeld, M. H., Berechid, B. E., Lopez, P. A., Meucci, O., McGlade, J. C., Rakic, P., and D'Adamio, L. (2002) *Proc. Natl. Acad. Sci. U. S. A.* **99,** 7102–7107
27. King, G. D., and Turner, S. R. (2004) *Exp. Neurol.* **185,** 208–219
28. Pedersen, W. A., Chan, S. L., Zhu, H., Abdur-Rahman, L. A., Verdi, J. M., and Mattson, M. P. (2002) *J. Neurochem.* **82,** 976–986
29. Chan, S. L., Pedersen, W. A., Zhu, H., and Mattson, M. P. (2002) *Neuromol. Med.* **1,** 55–67
30. Schmidlin, F., Dery, O., DeFea, K. O., Slice, L., Patierno, S., Sternini, C., Grady, E. F., and Bunnett, N. W. (2001) *J. Biol. Chem.* **276,** 25427–25437
31. Rebel, V. I., Tanaka, M., Lee, J.-S., Hartnett, S., Pulsipher, M., Nathan, D. G., Mulligan, R. C., and Sieff, C. A. (1999) *Blood* **93,** 2217–2224
32. Chan, S. L., Fu, W., Zhang, P., Lee, J., Cheng, A., Kokame, K., and Mattson, M. P. (2005) *J. Biol. Chem.* **279,** 28733–28743
33. Chan, S. L., Mayne, M., Holden, C. P., Geiger, J. D., and Mattson, M. P. (2000) *J. Biol. Chem.* **275,** 18195–18200
34. Wolfe, M. S. (2008) *Curr. Top. Med. Chem.* **8,** 2–8
35. Sever, S., Damke, H., and Schmid, S. L. (2000) *J. Cell Biol.* **150,** 1137–1148
36. Seugnet, B. L., Simpson, P., and Haenlin, M. (1997) *Dev. Biol.* **192,** 585–598
37. Ikin, A. F., Annaert, W. G., Takei, K., De Camilli, P., Jahn, R., Greengard, P., and Buxbaum, J. D. (1996) *J. Biol. Chem.* **271,** 31783–31786
38. Ferreira, A., Caceres, A., and Kosik, K. S. (1993) *J. Neurosci.* **13,** 3112–3123
39. Mattson, M. P., and Chan, S. L. (2001) *J. Mol. Neurosci.* **17,** 205–224
40. Caporaso, G. L., Takei, K., Gandy, S. E., Matteoli, M., Mundigl, O., Greengard, P., and De Camilli, P. (1994) *J. Neurosci.* **14,** 3122–3138
41. Beers, M. F. (1996) *J. Biol. Chem.* **271,** 14361–14370
42. Lai, E. C. (2002) *Curr. Biol.* **12,** 74–78
43. Fenteany, G., Standaert, R. F., Lane, W. S., Choi, S., Corey, E. J., and Schreiber, S. L. (1995) *Science* **268,** 726–731
44. Stein, B. S., Bensch, K. G, and Sussman, H. H. (1984) *J. Biol. Chem.* **259,** 14762–14772
45. Verdi, J. M., Bashirullah, A., Goldhawk, D. E., Kubu, C. J., Jamali, M., Meakin, S. O., and Lipshitz, H. D. (1999) *Proc. Natl. Acad. Sci. U. S. A.* **96,** 10472–10476
46. Bani-Yaghoub, M., Kubu, C. J., Cowling, R., Rochira, J., Nikopoulos, G. N., Bellum, S., and Verdi, J. M. (2007) *Dev. Dyn.* **236,** 696–705
47. Nie, J., McGill, M. A., Dermer, M., Dho, S. E., Wolting, C. D., and McGlade, C. J. (2002) *EMBO J.* **21,** 93–102
48. Susini, L., Passer, B. J., Amzallag-Elbaz, N., Juven-Gershon, T., Prieur, S., Privat, N., Tuynder, M., Gendron, M. C., Israël, A., Amson, R., Oren, M., and Telerman, A. (2001) *Proc. Natl. Acad. Sci. U. S. A.* **98,** 15067–15072
49. Juven-Gershon, T., Shifman, O., Unger, T., Elkeles, A., Haupt, Y., and Oren, M. (1998) *Mol. Cell. Biol.* **18,** 3974–3982
50. Zhou, M. M., Ravichandran, K. S., Olejniczak, E. F., Petros, A. M., Meadows, R. P., Sattler, M., Harlan, J. E., Wade, W. S., Burakoff, S. J., and Fesik S. W. (1995) *Nature* **378,** 584–592
51. Zwahlen, C., Li, S. C., Kay, L. E., Pawson, T., and Forman-Kay, J. D. (2000) *EMBO J.* **19,** 1505–1515
52. Li, S. C., Zwahlen, C., Vincent, S. J., McGlade, C. J., Kay, L. E., Pawson, T., and Forman-Kay, J. D. (1998) *Nat. Struct. Biol.* **5,** 1075–1083
53. Yaich, L., Ooi, J., Park, M., Borg, J. P., Landry, C., Bodmer, R., and Margolis, B. (1998) *J. Biol. Chem.* **273,** 10381–10388
54. Lu, B., Rothenberg, M., Jan, L. Y., and Jan, Y. N. (1998) *Cell* **95,** 225–235
55. Dho, S. E., Jacob, S., Wolting, C. D., French, M. B., Rohrschneider, L. R., and McGlade, C. J. (1998) *J. Biol. Chem.* **273,** 9179–9187
56. Di Marcotullio, L., Ferretti, E., Greco, A., De Smaele, E., Po, A., Sico, M. A., Alimandi, M., Giannini, G., Maroder, M., Screpanti, I., and Gulino, A. (2006) *Nat. Cell Biol.* **8,** 1415–1423
57. Lai, A., Sisodia, S. S., and Trowbridge, I. S. (1995) *J. Biol. Chem.* **270,** 3565–3573
58. Zmith, C. A., Dho, S. E., Donaldson, J., Tepass, U., and McGlade, C. J. (2004) *Mol. Biol. Cell* **15,** 3698–3708
59. D'Souza-Schorey, C., Li, G., Colombo, M. I., and Stahl, P. D. (1995) *Science* **267,** 1175–1178
60. Verbeek, M. M., Otte-Holler, I., Fransen, J. A., and deWaal, R. M. W. (2002) *J. Histochem. Cytochem.* **50,** 681–690

Numb Endocytic Adapter Proteins Regulate the Transport and Processing of the Amyloid Precursor Protein in an Isoform-dependent Manner: IMPLICATIONS FOR ALZHEIMER DISEASE PATHOGENESIS

George A. Kyriazis, Zelan Wei, Miriam Vandermey, Dong-Gyu Jo, Ouyang Xin, Mark P. Mattson and Sic L. Chan

J. Biol. Chem. 2008, 283:25492-25502.
doi: 10.1074/jbc.M802072200 originally published online July 2, 2008
